Supporting Information

Electrostatic vs Electronic interactions within oxidized multinuclear Pt(bipyridine)(dithiolene) complexes

Khalil Youssef, Antoine Vacher, Thanaphon Khrueawatthanawet, Thierry Roisnel , Frédéric Barrière, Dominique Lorcy*

Table of content

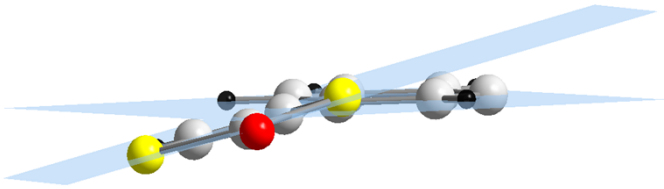

Fig. S1: Side view of 1,3-bis(dithiol-2-one) **3** with the central phenyl ring in the horizontal plane and the dithiole ring in the other one, the angle between the planes amounts to 14.2(2)°.

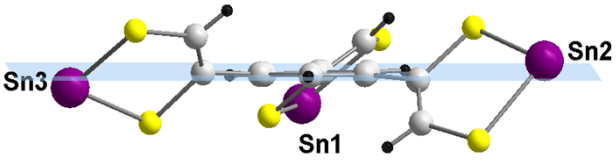

Fig. S2: Side view of compound **7** with the central phenyl ring in the horizontal plane showing the angles between the metalladithiolene planes and the phenyl ring plane rings in the range of 35.4(5)° - 49.1(3)°. Butyl chains have been omitted for clarity

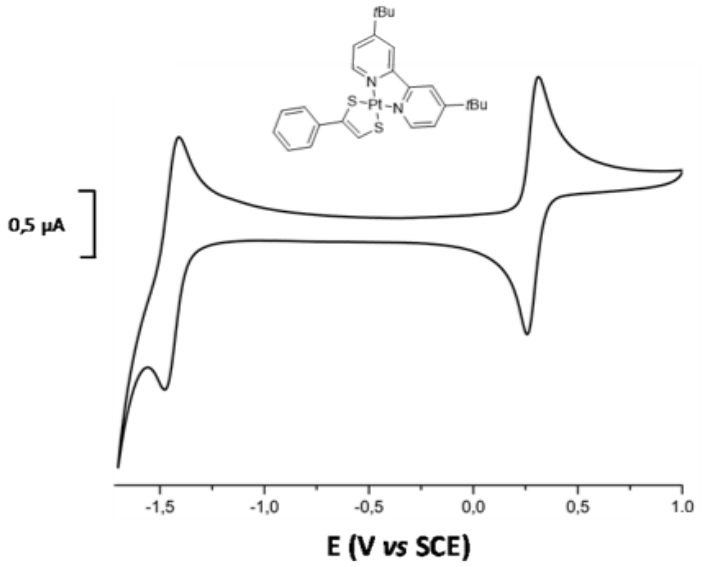

Fig. S3: Cyclic voltammogram of **PtP** in CH_2Cl_2 using 0.1 M of $[NBu_4][PF_6]$ as supporting electrolytes. v=100 $mV.s^{-1}$.

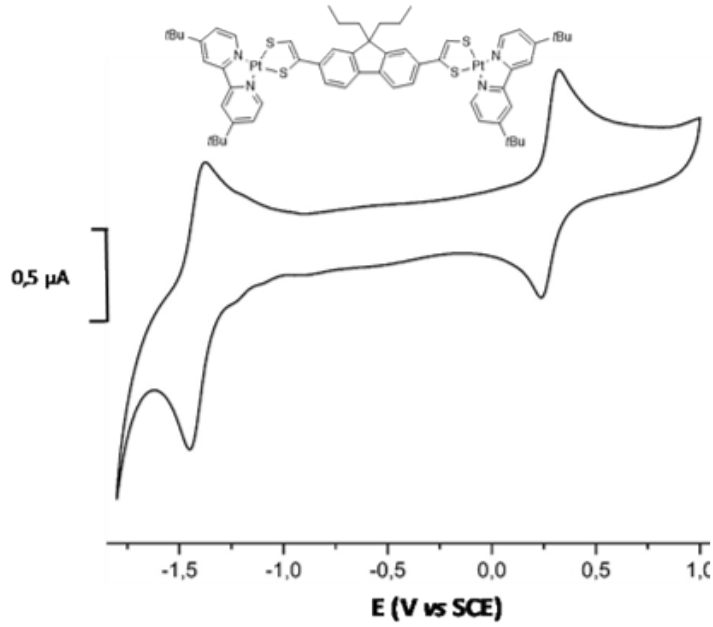

Fig. S4: Cyclic voltammogram of **Pt_2Fl** in CH_2Cl_2 using 0.1 M of $[NBu_4][PF_6]$ as supporting electrolytes. v=100 $mV.s^{-1}$.

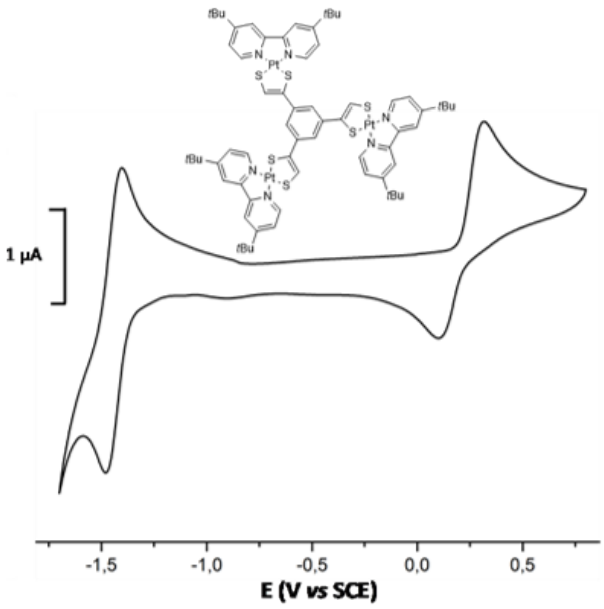

Fig. S5: Cyclic voltammogram of **$Pt_3$1,3,5-P** in CH_2Cl_2 using 0.1 M of $[NBu_4][PF_6]$ as supporting electrolytes. v=100 $mV.s^{-1}$.

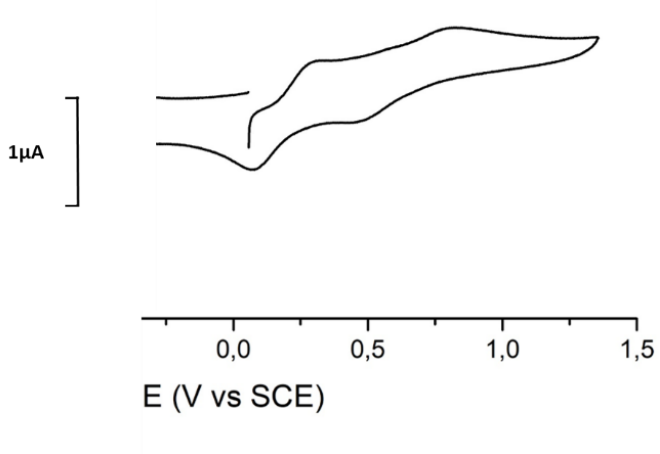

Fig. S6: Cyclic voltammogram of **$Pt_3$1,3,5-P** in CH_2Cl_2 using 0.005 M of $[NBu_4][BArF]$ as supporting electrolytes. v=100 $mV.s^{-1}$.

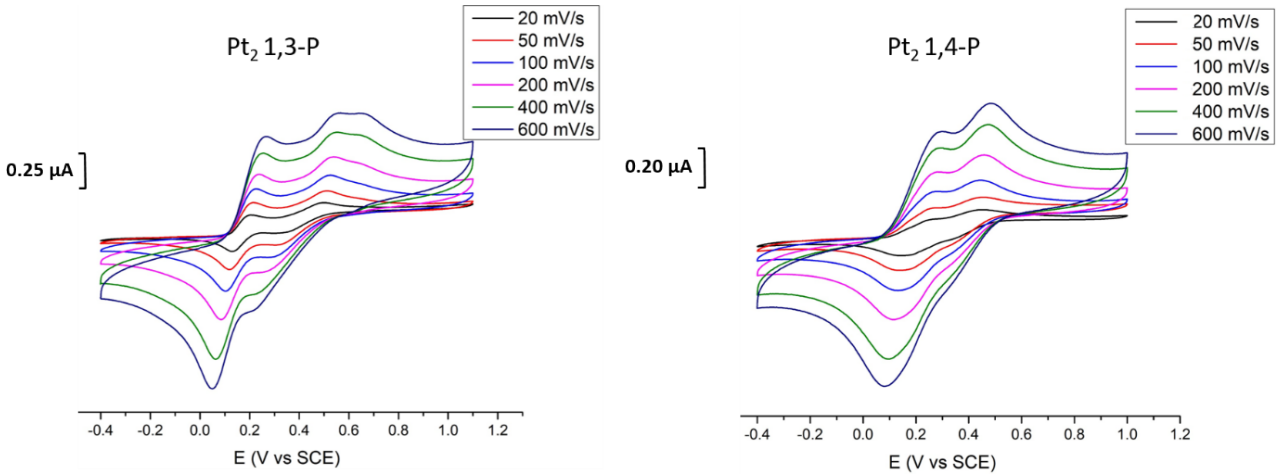

Fig. S7: Cyclic voltammogram of **$Pt_2$1,3-P** (left) and **$Pt_2$1,4-P** (right)in CH_2Cl_2 using 0.005 M of $[NBu_4][BArF]$ as supporting electrolytes. 20 mV/s<v<600 mV/s.

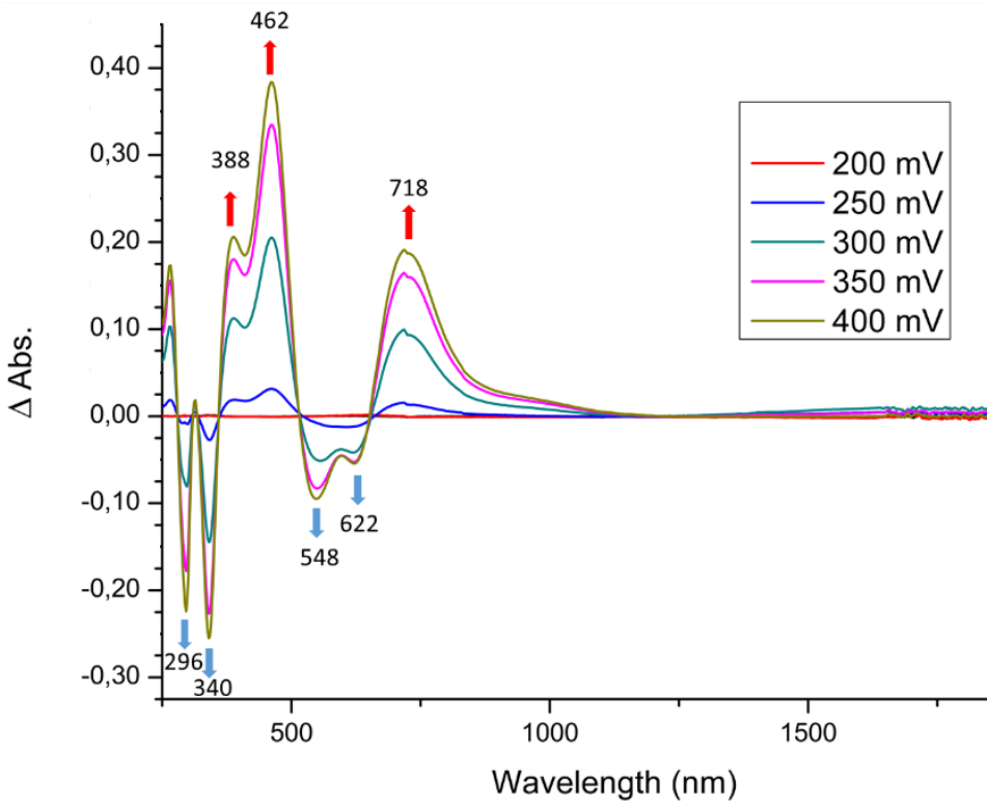

Fig. S8: Differential UV-vis-NIR spectra of **PtP** monitored upon gradual oxidation of the neutral complex with 0.2 M $[Bu_4N][PF_6]$ as the supporting electrolyte.

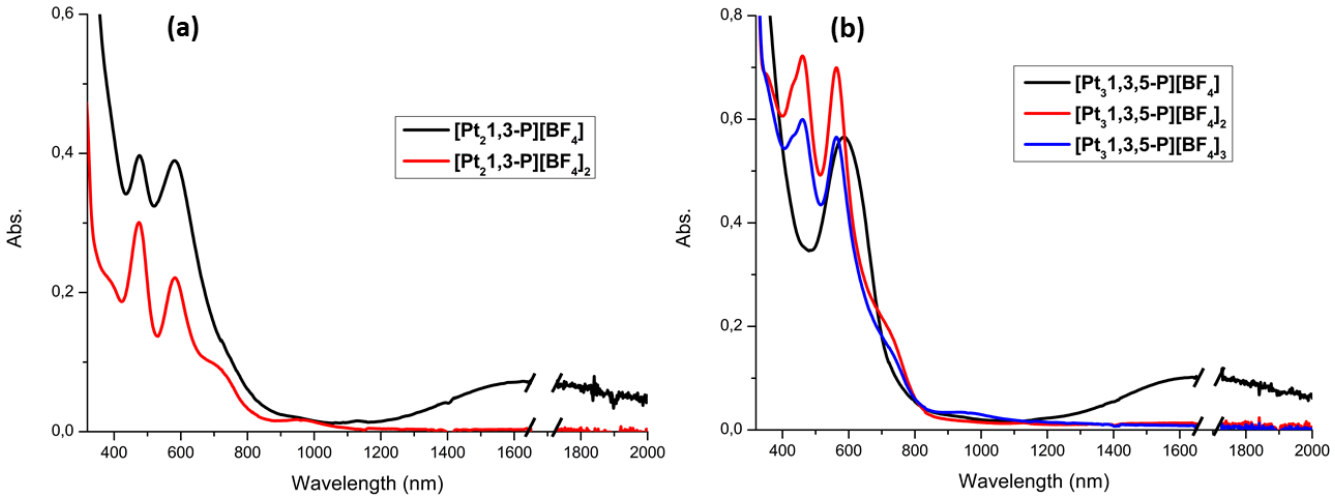

Fig. S9: UV-vis-NIR spectrum of Oxidized **$Pt_2$1,3-P** and **$Pt_3$1,3,5-P** complexes.

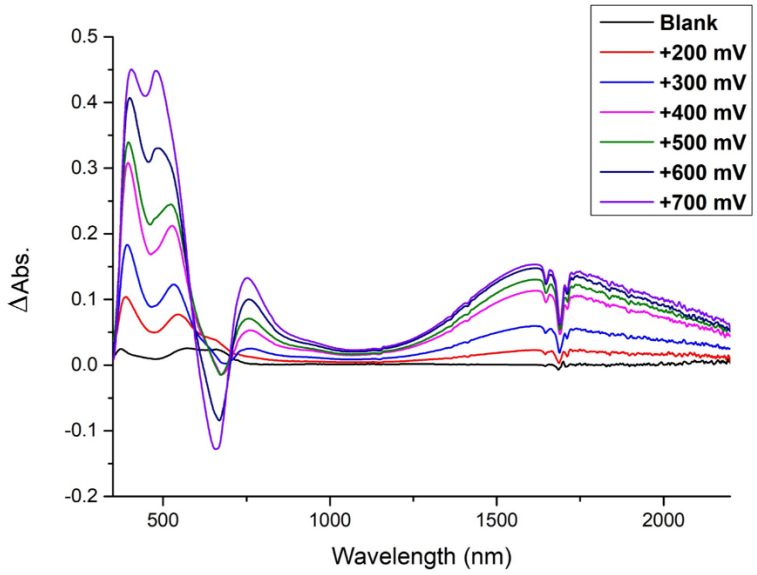

Fig. S10: Differential UV-vis-NIR spectra of **$Pt_3$1,3,5-P** monitored upon gradual oxidation of the neutral complex with 0.005 M [Bu_4N][BArF] as the supporting electrolyte.

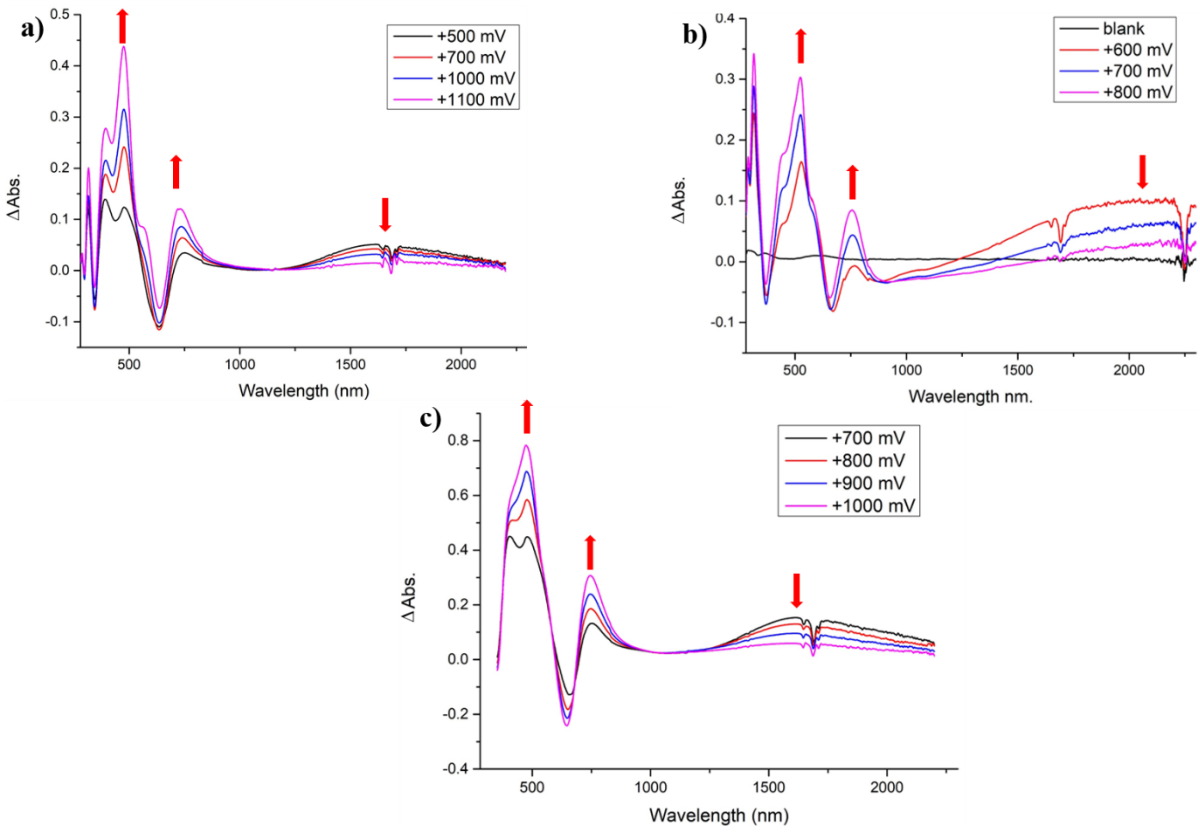

Fig. S11: Differential UV-vis-NIR spectra of **$Pt_2$1,3-P** (a), **$Pt_2$1,4-P** (b) and **$Pt_3$1,3,5-P** (c) monitored upon gradual oxidation with 0.005 M [Bu_4N][BArF] as the supporting electrolyte.

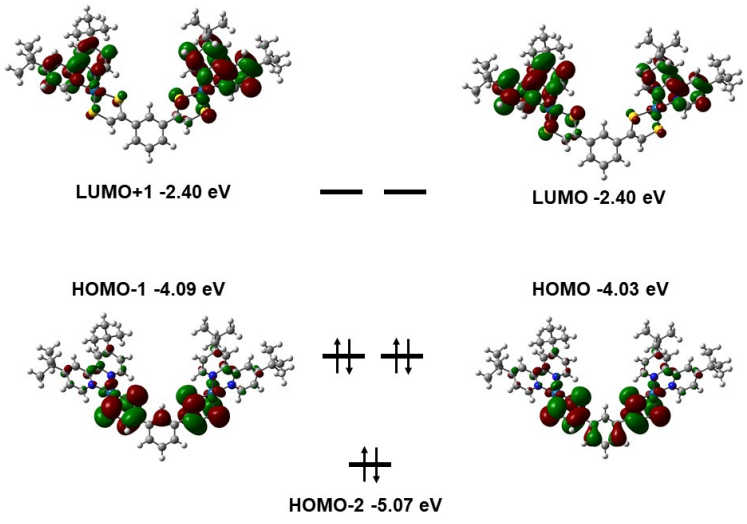

Fig. S12: Frontier molecular orbitals (HOMO, HOMO-1, LUMO and LUMO+1) and calculated energy levels for complex **Pt21,3-P**.

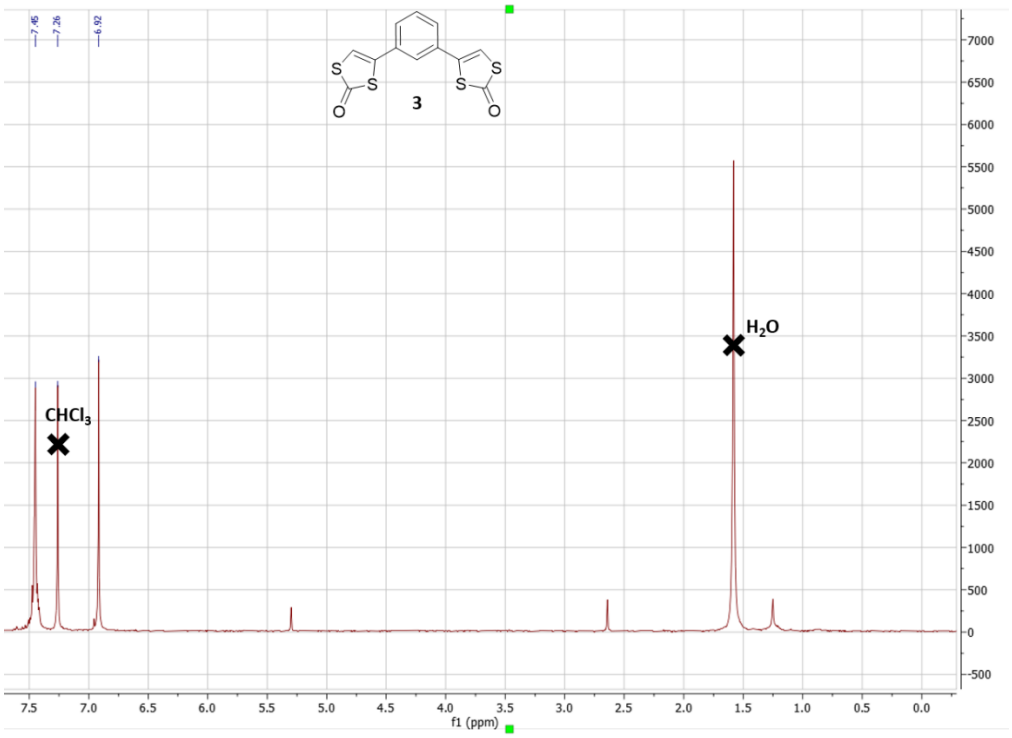

Fig. S13: ^{1}H RMN of **3**

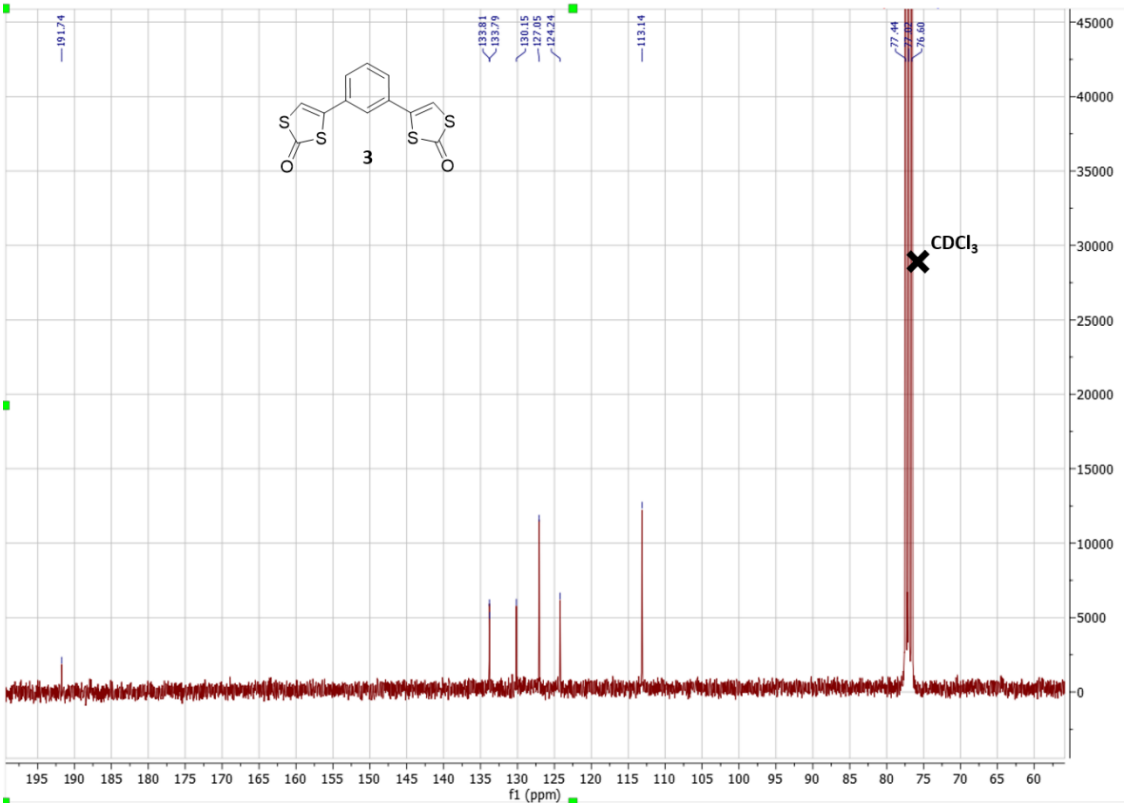

Fig. S14: ^{13}C RMN of **3**

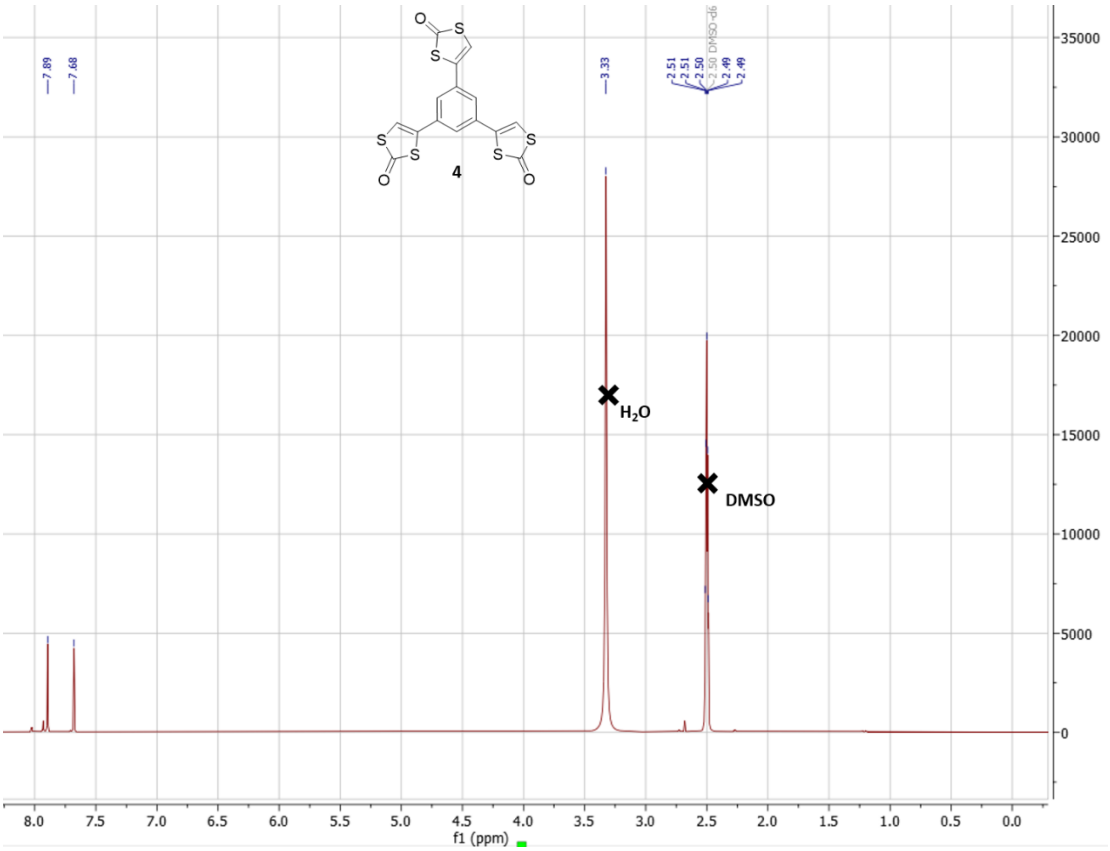

Fig. S15: ^{1}H RMN of **4**

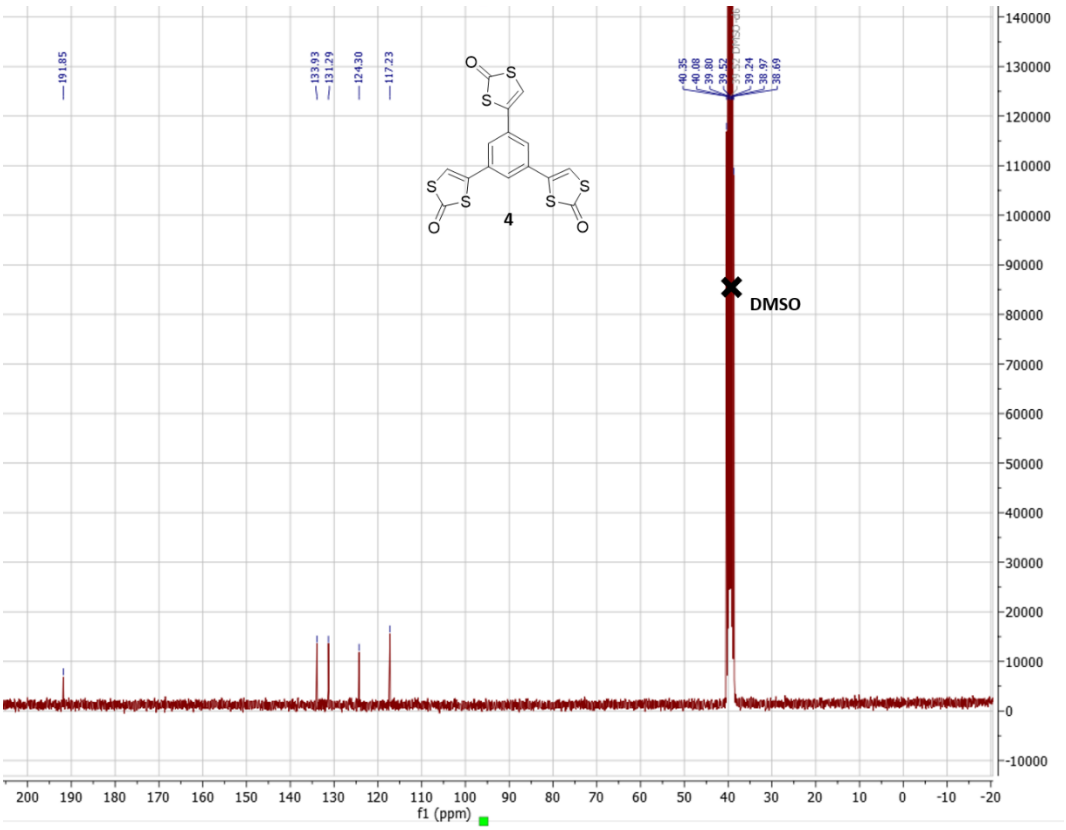

Fig. S16: ^{13}C RMN of **4**

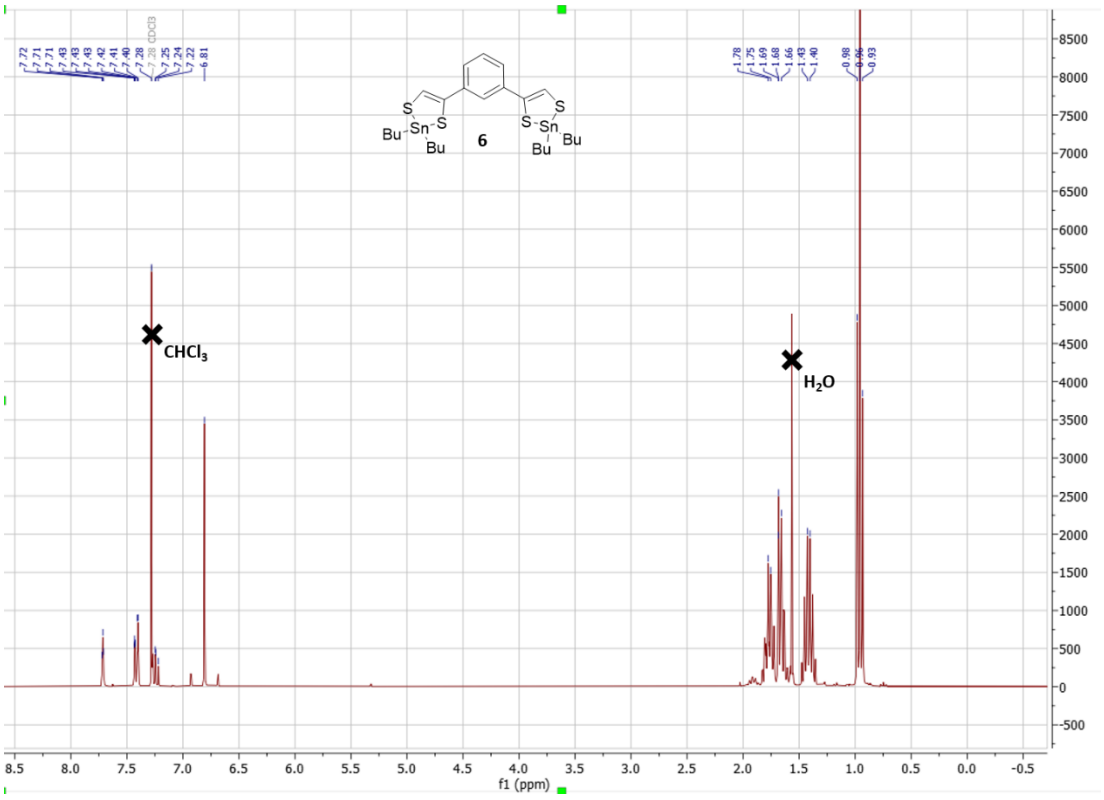

Fig. S17: ^{1}H RMN of **6**

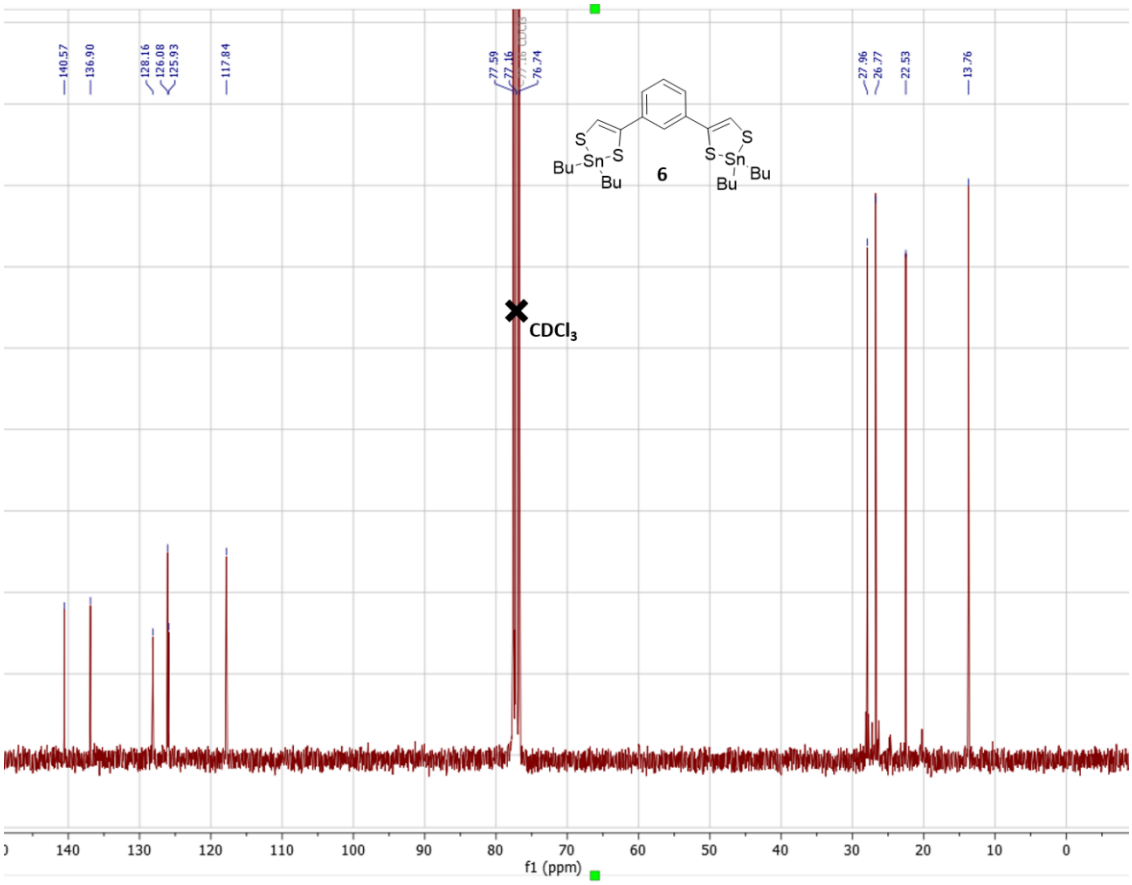

Fig. S18: ^{13}C RMN of **6**

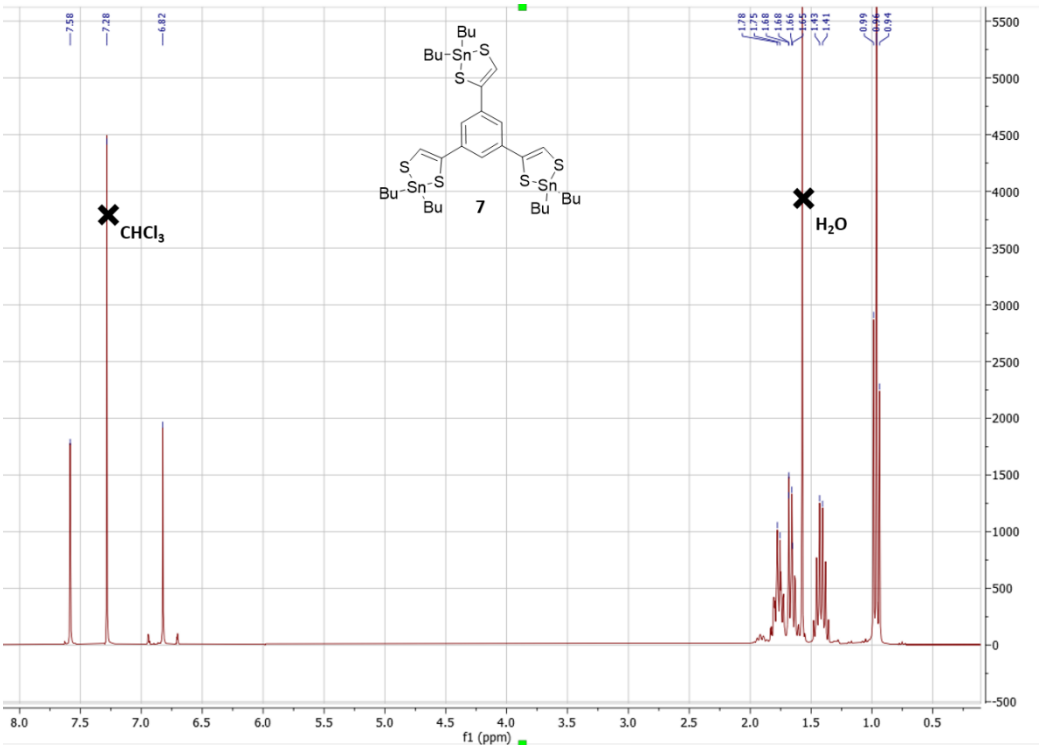

Fig. S19: ^{1}H RMN of **7**

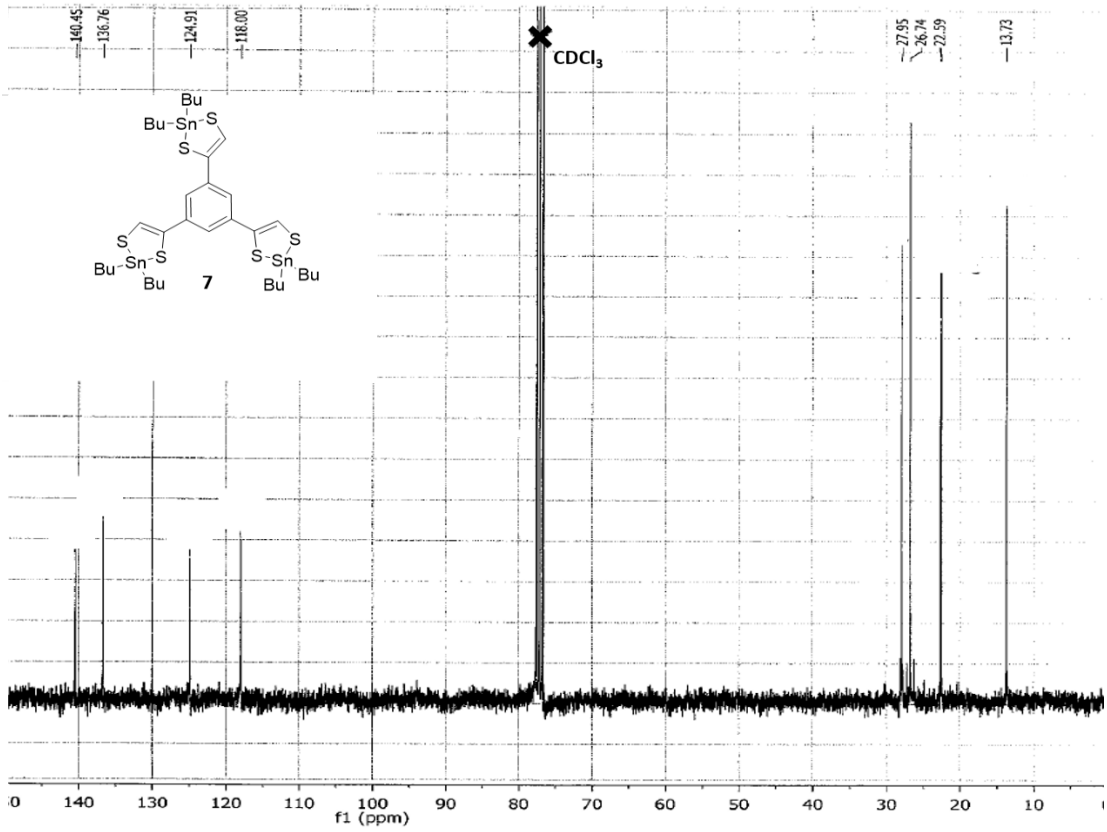

Fig. S20: ^{13}C RMN of **7**

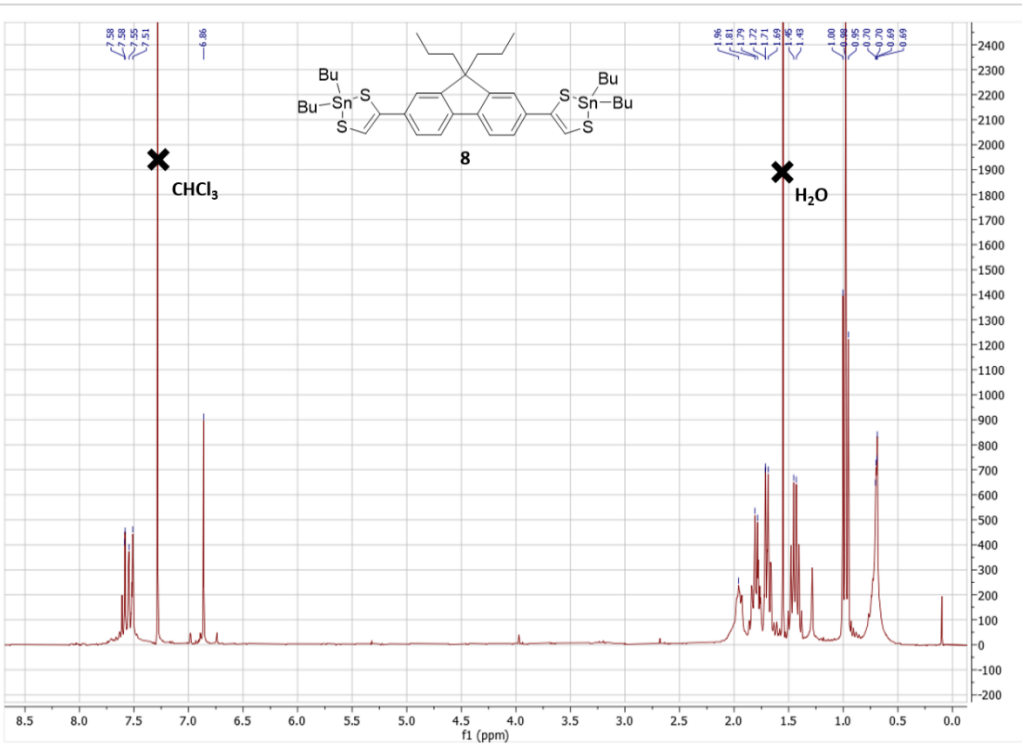

Fig. S21: ^{1}H RMN of **8**

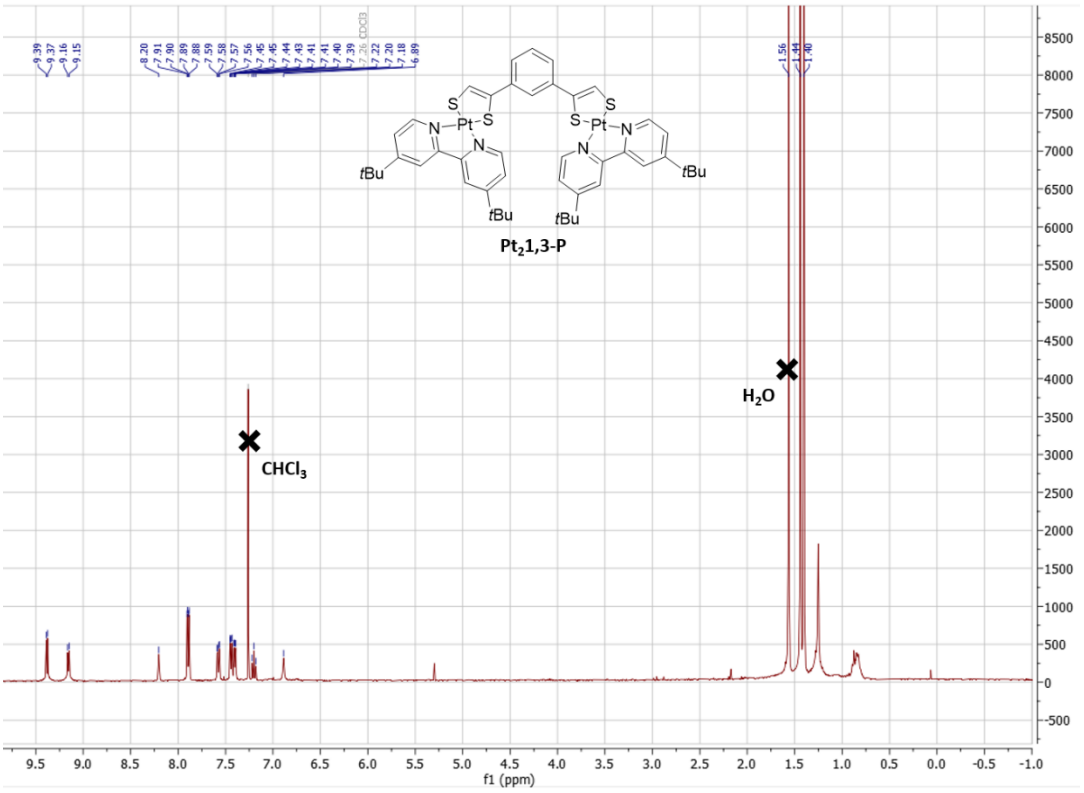

Fig. S22: ^{1}H RMN of **$Pt_2$1,3-P**

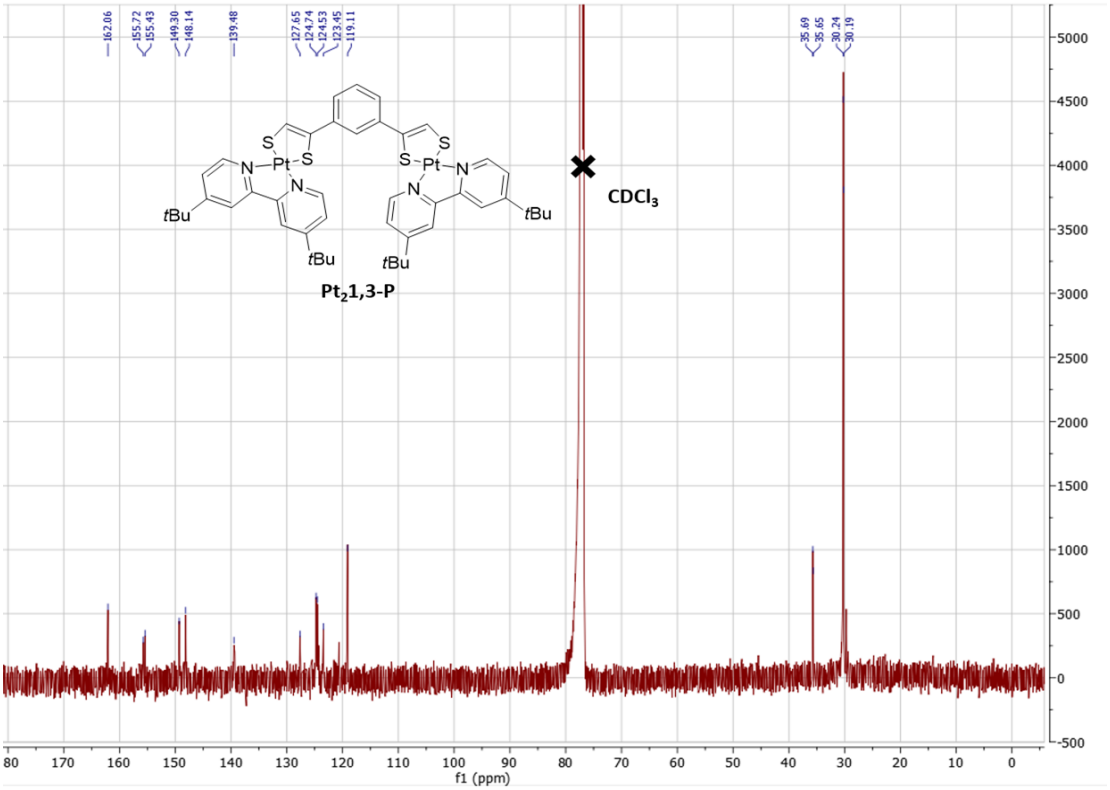

Fig. S23: ^{13}C RMN of **$Pt_2$1,3-P**

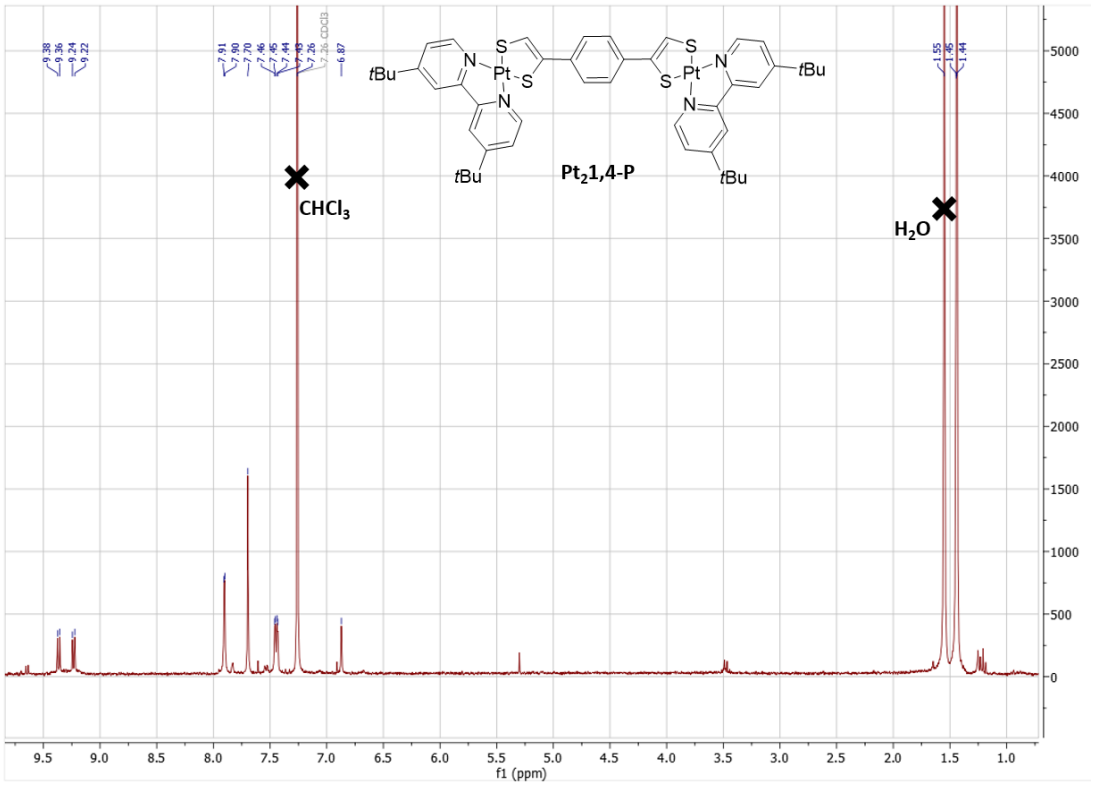

Fig. S24: ^{1}H RMN of **$Pt_2$1,4-P**

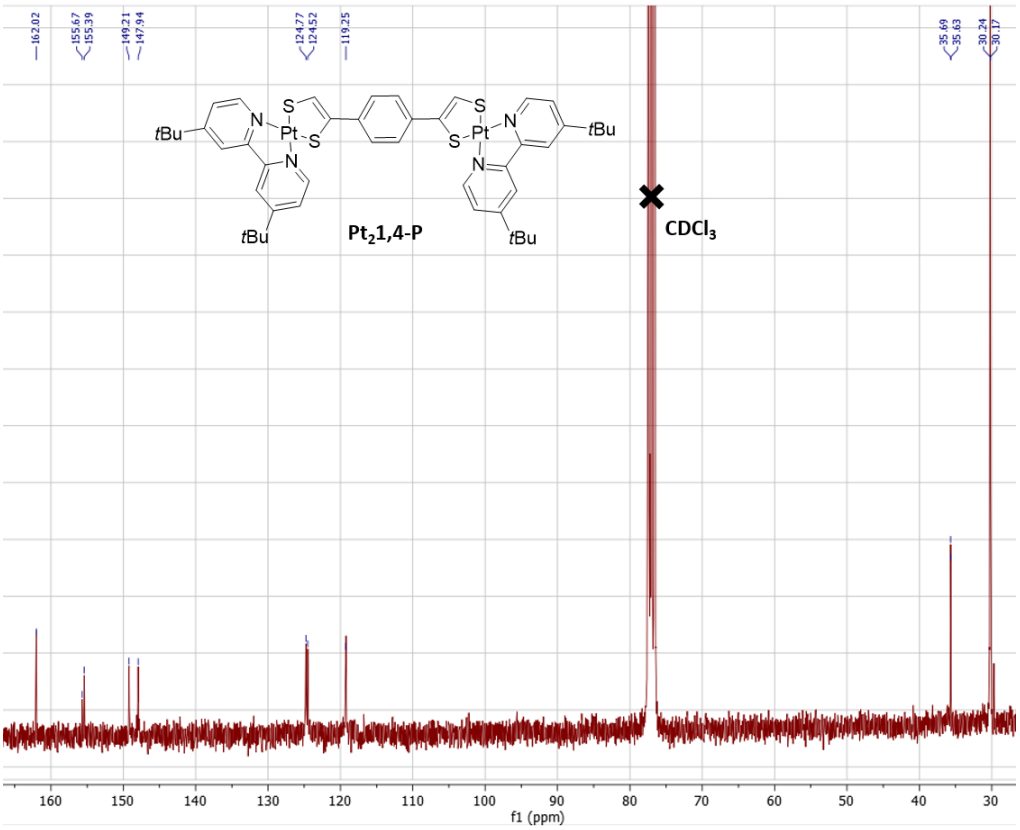

Fig. S25: ^{13}C RMN of **$Pt_2$1,4-P**

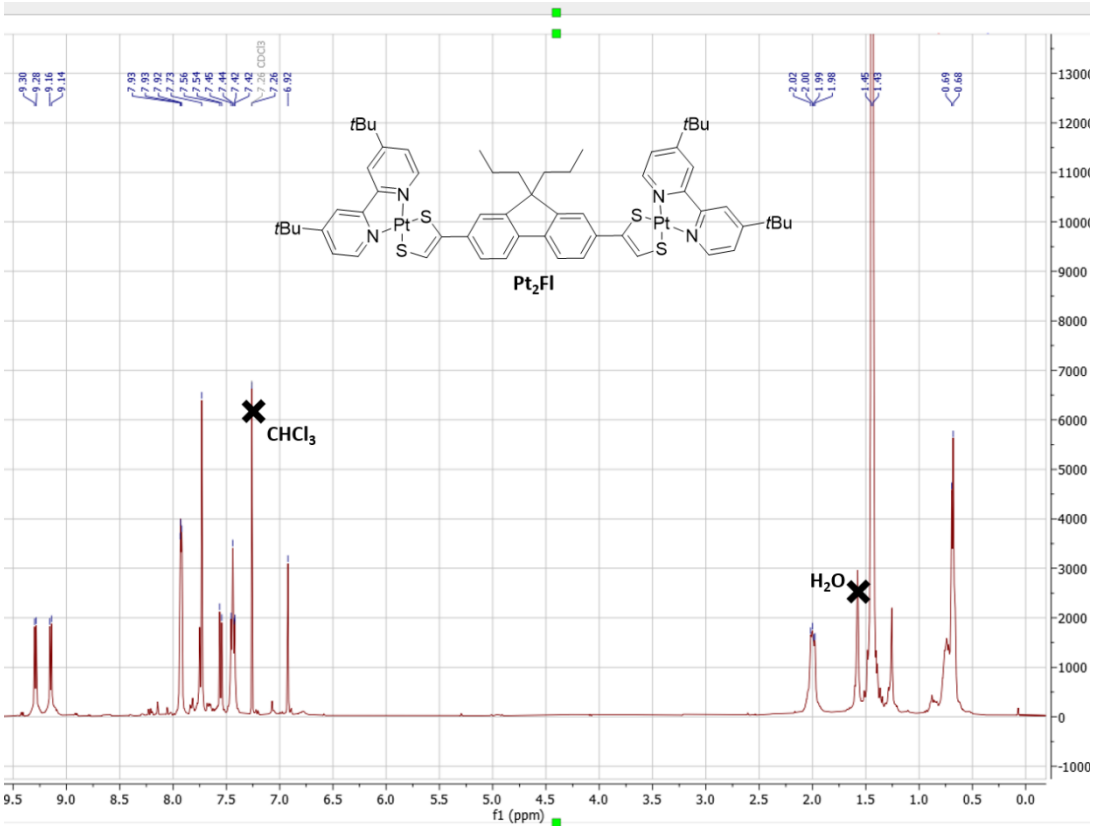

Fig. S26: ^{1}H RMN of **Pt_2Fl**

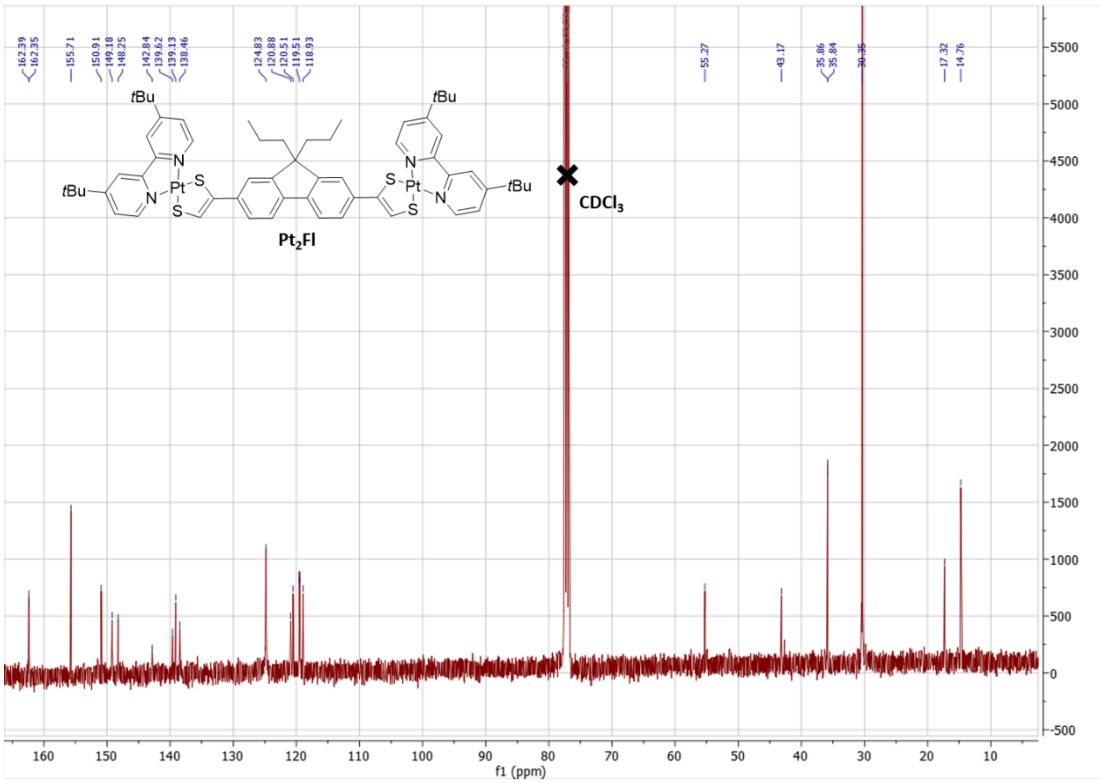

Fig. S27: ^{13}C RMN of **Pt_2Fl**

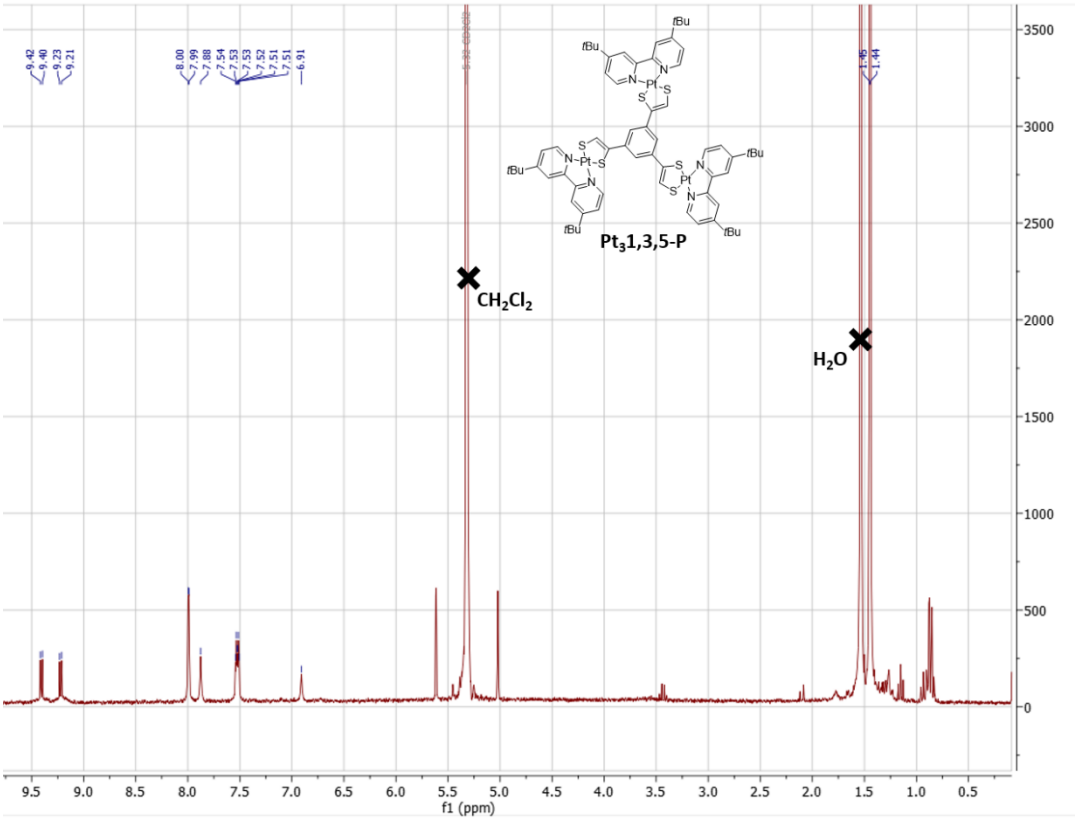

Fig. S28: ^{1}H RMN of **$Pt_3$1,3,5-P**